The impact of water storage capacity on plant dynamics in arid environments: a stoichiometric modeling approach

Cuihua Wang[a], Sanling Yuan[a,*], Hao Wang[b]

[a] *University of Shanghai for Science and Technology, Shanghai, 200093, China.*
[b] *Department of Mathematical and Statistical Sciences, University of Alberta, Edmonton, AB T6G2G1, Canada.*

Abstract

Plants in arid environments have evolved many strategies to resist drought. Among them, the developed water storage tissue is an essential characteristic of xerophytes. To clarify the role of water storage capacity in plant performance, we originally formulate a stoichiometric model to describe the interaction between plants and water with explicit water storage. Via an ecological reproductive index, we explore the effects of precipitation and water storage capacity on plant dynamics. The model possesses saddle-node bifurcation and forward or backward bifurcation, and the latter may lead to the emergence of alternative stable states between a stable survival state and a stable extinction state. Numerical simulations illustrate the persistence and resilience of plants regulated by soil conditions, precipitation and water storage capacity. Our findings contribute to the botanical theory in the perspectives of environmental change and plant water storage trait.

Keywords: Drought stress, Ecological stoichiometry, Model, Ecological reproductive index, Alternative stable states

---

1. Introduction

Arid and semi-arid regions are one of the most vulnerable regions in the world's ecosystems and water resource systems, as well as regions with the greatest variability in precipitation (Xu et al., 2021, Allen et al., 2015). Plants growing in this environment often encounter temporary or permanent drought stress, which severely restricts plant growth and distribution compared to other environmental factors, resulting in substantial productivity losses (Allen et al., 2010, 2015). In particular, in recent years, the increasing climate change has seriously affected the survival, growth, and evolution of plants, posing severe challenges to regional ecological construction and improvement of vegetation functions (Gustafson and Sturtevant, 2013).

Plants growing in arid and semi-arid environments generally have good adaptability to drought stress. They respond to drought to a certain extent, which is not caused by a s-

---

[*] Corresponding author
Email address: `sanling@usst.edu.cn` (Sanling Yuan)

ingle factor, but a comprehensive response generated by the interaction of multiple factors, mainly involving plant growth and development, morphological structure, drought stress signal transduction and drought stress gene expression regulation and other characteristics (Wei and Wang, 2015). These characteristics of plants are often referred to as drought resistance. Plants with strong drought resistance have some morphological or physiological characteristics, and the drought resistance of the same plant will change with season and age (DOdorico et al., 2019, Wei and Wang, 2015). In general, the adaptability of plants to the arid environments is mainly manifested in developed root systems, small leaf areas, developed water storage tissue, and high protoplasmic osmotic pressure (DOdorico et al., 2019).

It is generally known that plants need four suitable environmental factors for growth and reproduction: light, water, temperature, and nutrients. Drought may lead to stomatal closure, thereby reducing transpiration rates and limiting nutrient transport from roots to shoots. Therefore, drought stress can reduce the availability and transport of nutrients in soil substrates and plant tissues (Singh and Sale, 2000). Recently, some researchers have developed mathematical models to study the dynamics of nutrient cycles such as carbon, nitrogen (Manzoni et al., 2019), and phosphorus (Runyan and DOdorico, 2019) in drylands. Despite various reports on the effects of nutrient supply on plant growth, it is generally accepted that, under drought conditions, increasing nutrient supply does not improve plant growth if sufficient nutrients are already in the soil (Ahanger et al., 2016, Hu and Schmidhalter, 2005). On the contrary, soil water availability has been recognized as one of the main limiting factors for plant growth in arid regions (Snyder and Tartowski, 2006), which is affected by precipitation, infiltration, evaporation, transpiration, and soil drainage (Yin et al., 2019), and can also affect the occurrence and intensity of plant drought stress, and has an important impact on the net primary production capacity of the ecosystem (Yin et al., 2019).

Plants growing in arid environments generally have the ability to store a large amount of water in their bodies through various special tissues to maximize water retention and maintain their morphology. Compared with the water in the soil, the proportion of water in plants is also quite large (Waring and Running, 1978). Vacuoles are the water storage tissues of plants. The water storage capacity of plants varies with plant species, environmental conditions, age, etc. Different types of plants, as well as the same plant under different environmental conditions, different ages, and different organs have great differences in water content. For example, plants growing in hidden, moist environments have higher water content than those growing in sunny, dry environments; the active parts of plant life also have higher water content. This water source, that is, the water in plants is protected by plants and will not be affected by soil evaporation and competition for water between plants. Plants consume stored water through transpiration and replenish water storage through root absorption (Čermák et al., 2007). Transpiration demand and soil water availability jointly determine the storage and release mode of the water in plants. When transpiration demand is low and soil water availability is high, it is beneficial to water absorption and storage; With the increase of transpiration demand and the decrease of soil water availability, the water removal rate of leaves is higher than that of roots, so more stored water needs to be released to maintain transpiration. Under this strategy, plants can be supplied with water more stably, delaying the occurrence of drought stress and the corresponding closure of stomata. Hartzell et al. (2017) investigated a resistance-capacitance model, and they found that plant water storage may strongly affect plant growth performance by increasing carbon assimilation during the peak period of evaporation water demand and reducing plant water stress. It follows that water storage capacity of plants can play an important role in the plant performance in a water-limited ecosystem.

Under the condition that other factors are suitable, if water resources are sufficient and plant vacuoles are filled with water to fully swell, then the growth and development of plants are in the best state. If the water content of the vacuole is lower than that when it is fully expanded, there is a certain degree of water deficit and the plants will consume water from the soil, and if the plants cannot absorb water from the soil, they will start to consume the water previously stored in the plant tissues, if there has been no precipitation supplement, the plants will gradually stop growing or even wilt. Motivated by the idea of ecological stoichiometry (Loladze et al., 2000, Sterner and Elser, 2017, Wang et al., 2007), an approach that analyzes the constraints and consequences of mass balance of multiple chemical elements in ecological interactions, we mechanistically introduce a new variable (the water content in plants) and the Droop approach (different from the Monod approach in the literature) to explicitly describe the water storage in plants and the internal water-based growth following the same logic in Wang et al. (2022) that provided comprehensive comparisons and modeling guidance in using Monod and Droop forms. Our results show that for different types of soil, plants respond differently to the changes of environmental factors and plants' traits. Particularly, in sandy soils, plants are resilient to precipitation and water storage capacity.

The remaining parts of this paper are organized as follows. In Section 2, we propose a mathematical model with water storage capacity to describe the dynamics of soil water, water in plants, and plant biomass. The well-posedness of the model, and the qualitative analysis including the existence and stability of equilibria and related bifurcation analysis, are discussed in Section 3. Subsequently, we carry out some numerical simulations to illustrate the impact of precipitation and water storage capacity on the plant dynamics. Finally, we present some biological implications of our results.

2. Model Formulation

In this section, we formulate a coupled plant-water model to capture the growth dynamics of plants. We mainly focus on plants living in arid regions, where the solar radiation and mineral nutrients needed for the plant growth are assumed to be abundant, and the water is the only element limiting the growth of plants due to the particular climatic characteristics.

There are five categories for soil water: runway water, gravitational water, hygroscopic water, chemically combined water and capillary water. Among them only the capillary water is available to plants, which is the water that exists in the gaps between soil particles and can flow along the soil gaps. Plants absorb capillary water from the soil into the root xylem through root hairs during various processes such as respiration, transpiration, and infiltration. Noting that the dry weight of most organisms is mainly carbon (C), then we use carbon to characterize the plant density.

Three variables are introduced to describe the interaction between water and plants: the soil water content (W, kg H_2O/m^2), the water content in an individual plant (Q, kg H_2O/kg C), and the plant density (P, kg C/m^2). Here, the soil water is specifically referred to the water available to plants in the soil. In what follows, we will formulate our model by discussing the change rate of the three variables.

We first describe the change of the water content in a single plant. As noted, plants absorb water mainly through their roots, which are affected by root pressure and transpiration pull, as well as by external environmental factors such as the available water in the soil, soil aeration, and soil temperature. Also, plants capture carbon dioxide from the atmosphere for photosynthesis and loses water through transpiration. These biological processes work together to maintain the water balance in plants to meet the needs of plant survival and growth. Otherwise, plant water shortage may lead to leaf wilting, stomatal closure, photosynthesis reduction and protoplasm disorder. According to ecological stoichiometry, we denote the minimum and maximum water content in an individual plant by $Q_{\min}$ and $Q_{\max}$: at the level $Q = Q_{\max}$, the water available to the growth and development of plants is sufficient, in this case, the plants have the largest growth rate; at the level $Q = Q_{\min}$, the plants suffer from severe water shortage and thus the growth may cease. Therefore it can be seen that the water absorption by a single plant depends on the soil water content W, the water content in plants Q, and the water holding capacity $Q_{\max} - Q_{\min}$, and we assume that it takes the form of

$$\rho_{\max} \cdot \frac{Q_{\max} - Q}{Q_{\max} - Q_{\min}} \cdot \frac{W}{W + C}, \tag{2.1}$$

where $\rho_{\max}$ is the maximum water absorption rate of vegetation and the plant growth function for water takes the Monod form $\frac{W}{W+C}$, where C is the half-saturation constant. On the other hand, plants consume the water inside them through photosynthesis and convert it into the energy needed for growth. The per capita growth rate of plants is assumed to subject to the Droop form (Wang et al., 2022), which is an increasing function of the water content in a single plant Q:

$$\mu_{\max}\Big(1 - \frac{Q_{\min}}{Q}\Big), \tag{2.2}$$

where $\mu_{\max}$ is the maximum growth rate. Then the decreased water content in plants caused by the plant growth is $\mu_{\max}\big(1 - \frac{Q_{\min}}{Q}\big)Q$ and the growth rate of plants is $\mu_{\max}\big(1 - \frac{Q_{\min}}{Q}\big)P$.

For soil water, it is affected by precipitation (the only source of soil water), evaporation, and the absorption by the plant roots. The rainfall infiltrates into the soil and the infiltration rate of water $\mathcal{I}$ depends on the plant biomass and the soil conditions, i.e., there exists an infiltration feedback mechanism between plants and water (Gilad et al., 2004, Rietkerk et al., 2002, Gilad et al., 2007). Then the infiltration rate $\mathcal{I}$ can be writen as

$$\mathcal{I} = \alpha \frac{P + Bf}{P + B}, \tag{2.3}$$

where B means the speed at which the permeation rate reaches the maximum value α. $f \in [0, 1]$ characterizes the infiltration contrast for a specific soil: The smaller f is the higher the infiltration contrast is; specifically when $f = 1$ no infiltration feedback exists. The decrease of the soil water content includes two aspects: evaporation with a constant rate L and water absorption by the plant roots. The absorption rate of water by plants depends on the soil water content, the water potential difference inside and outside the roots of the plants and the plant biomass. Arguing as for (2.1), we know that the absorption rate of the soil water by plants is

$$\rho_{\max}\frac{Q_{\max}-Q}{Q_{\max}-Q_{\min}}\frac{WP}{W+C}. \tag{2.4}$$

For plants, they mainly absorb water, minerals and inorganic substances in the soil through their roots, and absorb carbon dioxide through their leaves. Through a series of life activities such as photosynthesis and respiration, the absorbed nutrients are converted into organic matter and stored in plants, and then continuous transformation and accumulation of organic matter enables plant cells to grow, divide, and finally achieve the growth of plants. In addition, more and more studies show that drought causes a large number of plant deaths worldwide (McDowell et al., 2008, Phillips et al., 2010). Climate change may make droughts more frequent and severe, and one concern is whether droughts will become more likely to induce the collapse of forest ecosystems. It is generally believed that the combined effects of drought and secondary disasters lead to large-scale tree death, and intraspecific competition is a very important factor. Here, we describe this loss of plants by crowding effect (quadratic mortality) and the mortality rate is assumed to be S. Disturbances other than water stress, such as storms, fires, pests or pathogens, can also cause plant mortality. We might as well call this mortality background mortality and assume the mortality rate to be M.

Assume the average daily precipitation is a constant A. Then, summarizing above, the mathematical model studied in this paper has the following form

$$\begin{aligned}
\frac{\mathrm{d}W}{\mathrm{d}t} &= \underbrace{\mathcal{I}A}_{\text{precipitation infiltration}} - \underbrace{LW}_{\text{evaporation and drainage}} - \underbrace{\rho_{\max}\frac{Q_{\max}-Q}{Q_{\max}-Q_{\min}}\frac{WP}{W+C}}_{\text{soil water loss due to plant absorption}},\\
\frac{\mathrm{d}Q}{\mathrm{d}t} &= \underbrace{\rho_{\max}\frac{Q_{\max}-Q}{Q_{\max}-Q_{\min}}\frac{W}{W+C}}_{\text{plant water absorption from soil}} - \underbrace{\mu_{\max}\left(1-\frac{Q_{\min}}{Q}\right)Q}_{\text{water loss in a single plant due to plant growth}},\\
\frac{\mathrm{d}P}{\mathrm{d}t} &= \underbrace{\mu_{\max}\left(1-\frac{Q_{\min}}{Q}\right)P}_{\text{plant growth limited by water}} - \underbrace{MP}_{\text{background mortality}} - \underbrace{SP^2}_{\text{crowding effect}}.
\end{aligned} \tag{2.5}$$

The state variables of model (2.5) are shown in Table 1. The values, interpretations, units and sources of parameters appearing in (2.5) are shown in Table 2.

Table 1: State variables of model (2.5).

Variable	Description	Units
W	Soil water content	kg H_2O/m^2
Q	Water content in a single plant	kg H_2O/kg C
P	Plant density	kg C/m^2

Model (2.5) is an ordinary differential equations describing the evolution of soil water, water in plants and the plant density. Considering the biological significance of these variables, we

Table 2: Parameters in model (2.5).

Parameter	Description	Value (Range)	Units	Sources
α	Infiltration rate in fully vegetated soil	40	1	Gilad et al. (2007)
A	Average precipitation rate	[0,1000]	kg H_2O/m^2/year	Gilad et al. (2007)
B	The rate at which the infiltration rate reaches the maximum value	0.05	kg C/m^2	Gilad et al. (2007)
f	Infiltration contrast between bare soil and vegetated soil	[0,1]	–	HilleRisLambers et al. (2001) Gilad et al. (2007)
L	Evaporation rate of soil water	4	year^{-1}	Gilad et al. (2007)
$\rho_{\max}$	Maximum soil water consumption rate	20	kg H_2O/kg C/year	HilleRisLambers et al. (2001)
$Q_{\max}$	Maximal water content in a single plant at which the water uptake ceases	[0.5,0.9]	kg H_2O/kg C	Default
$Q_{\min}$	Minimal water content in a single plant at which the plant growth ceases	[0.001,0.1]	kg H_2O/kg C	Default
C	Half saturation constant of specific plant growth and water uptake	5	kg H_2O/m^2	HilleRisLambers et al. (2001)
$\mu_{\max}$	Maximum vegetation specific production rate	0.032	year^{-1}	HilleRisLambers et al. (2001)
M	Background mortality rate of plants	1.2	year^{-1}	HilleRisLambers et al. (2001)
S	Specific loss rate of plant due to crowding effect	0.22	m^2 kg C/year	Gilad et al. (2007)

will discuss the solutions of model (2.5) with the initial values satisfying

$$W(0) \geq 0, Q_{\min} \leq Q(0) \leq Q_{\max}, P(0) \geq 0. \tag{2.6}$$

To facilitate mathematical analysis, we use the scaling listed in Table 3 to transform model (2.5)-(2.6) into the following nondimensionalized form

$$\begin{aligned}
\frac{\mathrm{d}w}{\mathrm{d}t} &= a\frac{p+f}{p+1} - lw - \gamma(\delta - q)\frac{wp}{w+1} := h_1(w,q,p),\\
\frac{\mathrm{d}q}{\mathrm{d}t} &= \beta(\delta - q)\frac{w}{w+1} - c(q-1) := h_2(w,q,p),\\
\frac{\mathrm{d}p}{\mathrm{d}t} &= c\Big(1 - \frac{1}{q}\Big)p - p - sp^2 := h_3(w,q,p)
\end{aligned} \tag{2.7}$$

with initial value

$$w(0) \geq 0,\ 1 \leq q(0) \leq \delta,\ p(0) \geq 0, \tag{2.8}$$

where we still use t by replacing t'. For the simplification of notation, denote

$$\mathcal{G} := \mathbb{R}_+ \times [1,\delta] \times \mathbb{R}_+. \tag{2.9}$$

Obviously, $(w(0), q(0), p(0)) \in \mathcal{G}$ if and only if it satisfies (2.8). Thus we need only to consider model (2.7) with initial values in $\mathcal{G}$.

Notice that plants can survive successfully in bare soil only if their growth rate exceeds the loss rate; otherwise they will die. Therefore, in this paper, we always assume that $\mu_{\max} > M$ in model (2.5), i.e., $c > 1$ in model (2.7).

Table 3: Relations between non-dimensional variables and parameters, and the dimensional ones appearing in (2.5) and (2.7).

Quantity	Scaling	Quantity	Scaling
w	$\frac{W}{C}$	γ	$\frac{B\rho_{\max}}{CM(\delta-1)}$
q	$\frac{Q}{Q_{\min}}$	β	$\frac{\rho_{\max}}{MQ_{\min}(\delta-1)}$
p	$\frac{P}{B}$	c	$\frac{\mu_{\max}}{M}$
δ	$\frac{Q_{\max}}{Q_{\min}}$	s	$\frac{SB}{M}$
a	$\frac{A\alpha}{MC}$	l	$\frac{L}{M}$
t'	Mt		

3. Model dynamics

3.1. Feasible domain

Our first theorem states the well-posedness of model (2.7).

Theorem 3.1. *Any solution of model* (2.7) *starting from* $\mathcal{G}$ *remains in it for all* $t \geq 0$. *Moreover, they are uniformly ultimately bounded.*

Proof. We first show that $\mathcal{G}$ is positively invariant for model (2.7). Obviously, the vector valued function (h_1, h_2, h_3) defined in model (2.7) is continuous and local Lipschizian with respect to (w, q, p) in $\mathcal{G}$. Notice from the third equation of p in model (2.7) that $p = 0$ is a solution of model (2.7). According to the existence and uniqueness theorem of solutions for ordinary differential equations, any solution starting from $\mathcal{G}$ cannot leave it by crossing the coordinate plane $p = 0$. It then follows from the first equation of w in model (2.7) that

$$\frac{\mathrm{d}w}{\mathrm{d}t}\bigg|_{w=0} = a\frac{p+f}{p+1} > 0, \tag{3.1}$$

which means that any solution starting from $\mathcal{G}$ with $w(0) = 0$ will enter the interior of $\mathcal{G}$. Notice further from the second equation of q in model (2.7) that

$$\frac{\mathrm{d}q}{\mathrm{d}t}\bigg|_{q=1} = \beta\delta\frac{w}{w+1} \geq 0 \quad \text{and} \quad \frac{\mathrm{d}q}{\mathrm{d}t}\bigg|_{q=\delta} = -c(\delta-1) < 0. \tag{3.2}$$

Thus we can conclude that for any solution of model (2.7) starting with the initial value in $\mathcal{G}$, it will remain in the region.

Now we are in a position to prove that all solutions starting from $\mathcal{G}$ are uniformly ultimately bounded. Define

$$N = pq + \frac{\beta}{\gamma}w. \tag{3.3}$$

Then we can compute that

$$\begin{aligned}\frac{\mathrm{d}N}{\mathrm{d}t} &= -lN + (l-1)pq - sp^2q + \frac{a\beta(p+f)}{\gamma(p+1)} \\ &\le -lN + (l-1)pq - sp^2q + \frac{a\beta}{\gamma} \\ &\le -lN + \frac{(l-1)^2q}{4s} + \frac{a\beta}{\gamma} \\ &\le -lN + \frac{(l-1)^2\delta}{4s} + \frac{a\beta}{\gamma},\end{aligned}$$

which implies that

$$\limsup_{t\to\infty} N(t) \le \frac{(l-1)^2\delta}{4ls} + \frac{a\beta}{l\gamma}. \tag{3.4}$$

Thus all solutions of model (2.7) with initial values in $\mathcal{G}$ are ultimately bounded and therefore exist globally for all $t \ge 0$. □

Denote

$$\Omega = \left\{(w,q,p) \in \mathcal{G} \middle| pq + \frac{\beta}{\gamma}w \le \frac{(l-1)^2\delta}{4ls} + \frac{a\beta}{l\gamma}\right\}. \tag{3.5}$$

Then Ω is a globally attracting region of model (2.7) with initial values in $\mathcal{G}$.

3.2. Ecological reproductive index

The viability of plants can be characterized by the ecological reproductive index, which is defined for model (2.7) by

$$\mathcal{R}_0 = \frac{\beta caf(\delta-1)}{\beta\delta af + caf + cl}. \tag{3.6}$$

In terms of the original parameters in model (2.5), $\mathcal{R}_0$ can be written as

$$\mathcal{R}_0 = \mu_{\max}\left(1 - \frac{Q_{\min}}{\widetilde{Q}}\right) \cdot \frac{1}{M}, \tag{3.7}$$

where

$$\widetilde{Q} = \frac{\rho_{\max}\frac{Q_{\max}}{Q_{\max}-Q_{\min}} + \mu_{\max}Q_{\min}}{\mu_{\max} + \frac{\rho_{\max}}{Q_{\max}-Q_{\min}}\frac{\frac{\alpha fA}{L}}{\frac{\alpha fA}{L}+C}}$$

is the water content in a single plant at the 'zero-vegetation' equilibrium state $(\frac{\alpha fA}{L}, \widetilde{Q}, 0)$; $\frac{1}{M}$ is the average life span of plants. Biologically, $\mathcal{R}_0$ characterizes the average amount of new plants produced by one unit plants during the average life span of plants.

Remark 3.2. *$\mathcal{R}_0$ can be obtained by analyzing the stability of 'zero-vegetation' equilibrium state, which is shown in Appendix A. From* (3.6)*, we can see that increasing water storage capacity of plants δ or precipitation a, improving the soil condition f, and reducing the loss rate of soil water l can enhance the colonized rate of plants in the bare soils.*

3.3. Existence and stability of equilibria

Notice from (3.5) that all the equilibria of model (2.7) should lie in the region Ω and can be determined by solving

$$a\frac{p+f}{p+1} - lw - \gamma(\delta - q)\frac{wp}{w+1} = 0, \tag{3.8}$$

$$\beta(\delta - q)\frac{w}{w+1} - c(q-1) = 0, \tag{3.9}$$

$$c\Big(1 - \frac{1}{q}\Big)p - p - sp^2 = 0. \tag{3.10}$$

Clearly, model (2.7) always possesses a 'no-vegetation' equilibrium $E^0(w^0, q^0, 0)$, where

$$w^0 = \frac{af}{l}, \quad q^0 = 1 + \frac{\beta af(\delta - 1)}{lc + (\beta + c)af}. \tag{3.11}$$

In the following, we try to find other nonnegative equilibria with $p \neq 0$. Notice from (3.10) that if $0 < p < \frac{c-1}{s}$, we have

$$q = \frac{c}{c - 1 - sp}. \tag{3.12}$$

Substituting (3.12) into (3.9), we obtain that if $\delta > \frac{c(\beta+1)}{(c-1)\beta}$ and $0 < p < \widehat{p} := \frac{\beta\delta(c-1) - \beta c - c}{(\beta\delta + c)s}$, then,

$$w = \frac{c(1 + sp)}{\beta\delta(c - 1 - sp) - \beta c - c(1 + sp)}. \tag{3.13}$$

It is easy to check that $\widehat{p} < \frac{c-1}{s}$. Thus, we only need to pay our attention to the range $p \in I := (0, \widehat{p})$ under conditions $\delta > \frac{c(\beta+1)}{(c-1)\beta}$ and $c > 1$. By substituting (3.12) and (3.13) into (3.8), we obtain the following equality

$$\frac{a(p+f)}{(1+p)(1+sp)} = \frac{lc}{\beta\delta(c - 1 - sp) - \beta c - c(1 + sp)} + \frac{c\gamma p}{\beta(c - 1 - sp)}. \tag{3.14}$$

For the convenience of analysis, we respectively denote the expressions on the left and right side of (3.14) as $F(p)$ and $G(p)$. Then the positive roots of (3.14) can be determined by looking for the intersection point of function curves of $F(p)$ and $G(p)$ in the range $p \in I$.

For the function $F(p)$, its derivative has the form

$$F'(p) = \frac{a\big(-sp^2 - 2sfp + 1 - f(s+1)\big)}{(sp^2 + (s+1)p + 1)^2}.$$

By a direct computation, we can find that when $f < \frac{1}{s+1}$, there exists a positive number

$$\tilde{p} = \frac{2sf - \sqrt{4s(f-1)(sf-1)}}{-2s}$$

such that $F'(p) > 0$ for $0 < p < \tilde{p}$ and $F'(p) < 0$ for $p > \tilde{p}$; while when $f > \frac{1}{s+1}$, $F'(p) < 0$ for all $p > 0$.

Similarly, the derivative of $G(p)$ indicates that $G(p)$ is a continuous and increasing function in the interval I. In addition, by taking the second derivative of $G(p)$, we have

$$G''(p) = \frac{2lcs(\beta\delta + c)^2}{\big(\beta\delta(c-1-sp) - \beta c - c(1+sp)\big)^3} + \frac{2c\gamma s(c-1)}{\beta(c-1-sp)^3}. \tag{3.15}$$

It is easy to see that $G''(p) > 0$ for $p \in I$, which indicates that $G(p)$ is also convex increasing. Notice also that

$$F(0) = af,\ \lim_{p\to\infty} F(p) = 0,\ G(0) = \frac{lc}{\beta\delta(c-1) - \beta c - c} > 0,\ \lim_{p\to\frac{\beta\delta(c-1)-\beta c-c}{(\beta\delta+c)s}} G(p) = \infty. \tag{3.16}$$

Combining the properties of these two functions $F(p)$ and $G(p)$ for $p \in I$, we can obtain the following results:

(i) if $f < \frac{1}{s+1}$ and $\delta > \frac{c(\beta+1)}{(c-1)\beta}$, then when $a > \frac{lc}{f(\beta\delta(c-1)-\beta c-c)}$, the functions $F(p)$ and $G(p)$ have a unique intersection point in I; when $a < \frac{lc}{f(\beta\delta(c-1)-\beta c-c)}$, the two functions may have none, one or two intersection point in I;

(ii) if $f > \frac{1}{s+1}$ and $\delta > \frac{c(\beta+1)}{(c-1)\beta}$, then when $a \geq \frac{lc}{f(\beta\delta(c-1)-\beta c-c)}$, then the functions $F(p)$ and $G(p)$ have a unique intersection point in I; when $a < \frac{lc}{f(\beta\delta(c-1)-\beta c-c)}$, then the two functions have no intersection points in I.

Then, summarizing, we obtain the following theorem about the existence of equilibria of model (2.7).

Theorem 3.3. *Model* (2.7) *always exists a 'no-vegetation' equilibrium* $E^0(w^0, q^0, 0)$, *where*

$$w^0 = \frac{af}{l}, \quad q^0 = 1 + \frac{\beta af(\delta-1)}{lc + (\beta+c)af}.$$

Moreover, if $\delta > \frac{c(\beta+1)}{(c-1)\beta}$ *and* $c > 1$ *are satisfied, then*

(1) when $\mathcal{R}_0 > 1$, *then model* (2.7) *has a unique positive equilibrium;*

(2) when $\mathcal{R}_0 < 1$, *then model* (2.7) *has none, one or two positive equilibria.*

We now begin to study the stability of equilibria with respect to spatially homogeneous perturbations. For this purpose, we discuss the Jacobi matrix of model (2.7), which is given by

$$J(E) = \begin{pmatrix} -l - \frac{\gamma(\delta-q)p}{(w+1)^2} & \frac{\gamma wp}{w+1} & \frac{a(1-f)}{(p+1)^2} - \frac{\gamma(\delta-q)w}{w+1} \\ \frac{\beta(\delta-q)}{(w+1)^2} & -\frac{\beta w}{w+1} - c & 0 \\ 0 & \frac{cp}{q^2} & c(1-\frac{1}{q}) - 1 - 2sp \end{pmatrix} := \begin{pmatrix} a_{11} & a_{12} & a_{13} \\ a_{21} & a_{22} & 0 \\ 0 & a_{32} & a_{33} \end{pmatrix}, \tag{3.17}$$

where (w, q, p) is any constant steady state of model (2.7).

For the boundary equilibrium $E^0(w^0, q^0, 0)$, the eigenvalues of Jacobi matrix $J(E^0)$ are

$$\lambda_1 = -l < 0, \quad \lambda_2 = -\frac{\beta a f}{af + l} - c < 0, \quad \lambda_3 = \mathcal{R}_0 - 1. \tag{3.18}$$

Then the stability of $E^0(w^0, q^0, 0)$ is governed by λ_3, which is locally asymptotically stable if $\mathcal{R}_0 < 1$ and unstable if $\mathcal{R}_0 > 1$.

Notice that $\mathcal{R}_0 < 1$ implies that $1 < \delta < \frac{c}{c-1} \cdot \frac{\beta af + af + l}{\beta af}$ for which E^0 is locally asymptotically stable with respect to spatially homogeneous perturbations. If δ is further restricted in the range $1 < \delta < \frac{c}{c-1}$, then E^0 is also globally asymptotically stable (see Appendix B for the proof).

Lemma 3.4. *Assume that* $1 < \delta < \frac{c}{c-1}$ *and* $c > 1$. *Then for model* (2.7), *the 'zero-vegetation' uniform state* $E^0(w^0, q^0, 0)$ *is globally asymptotically stable.*

For the positive equilibrium $E^*(w^*, q^*, p^*)$, if exists, the corresponding characteristic equation is

$$\lambda^3 - \mathrm{Tr}_0\lambda^2 - h_0\lambda - \mathrm{Det}_0 = 0, \tag{3.19}$$

where

$$\begin{aligned}
\mathrm{Tr}_0 =& - l - \frac{\gamma(\delta - q)p^*}{(w^* + 1)^2} - \frac{\beta w^*}{w^* + 1} - c - sp^* < 0,\\
h_0 =& - sp^*\Big(l + \frac{\gamma(\delta - q^*)p^*}{(w^* + 1)^2} + \frac{\beta w^*}{w^* + 1} + c\Big) - l\Big(\frac{\beta w^*}{w^* + 1} + c\Big) - \frac{\gamma c(\delta - q^*)p^*}{(w^* + 1)^2} < 0,\\
\mathrm{Det}_0 =& - sp^*\Big(l\Big(\frac{\beta w^*}{w^* + 1} + c\Big) + \frac{\gamma c(\delta - q^*)p^*}{(w^* + 1)^2}\Big) - \frac{c\beta\gamma(\delta - q^*)^2 p^* w^*}{q^{*2}(w^* + 1)^3} + \frac{ac\beta(1 - f)(\delta - q^*)p^*}{q^{*2}(w^* + 1)^2(p^* + 1)^2},
\end{aligned}$$

and

$$\begin{aligned}
\mathrm{Tr}_0 h_0 + \mathrm{Det}_0 =& sp^* l\Big(l + \frac{\gamma(\delta - q^*)p^*}{(w^* + 1)^2} + sp^*\Big) + \frac{\gamma s(\delta - q^*)p^{*2}}{(w^* + 1)^2}\Big(l + sp^* + \frac{\gamma(\delta - q^*)p^*}{(w^* + 1)^2} + \frac{\beta w^*}{w^* + 1}\Big)\\
&+ \Big(\frac{\beta sp^* w^*}{w^* + 1} + scp^* + \frac{\beta l w^*}{w^* + 1} + cl + \frac{\gamma c(\delta - q^*)p^*}{(w^* + 1)^2}\Big)\Big(l + c + sp^* + \frac{\gamma(\delta - q^*)p^*}{(w^* + 1)^2}\\
&+ \frac{\beta w^*}{w^* + 1}\Big) - \frac{c\beta\gamma(\delta - q^*)^2 p^* w^*}{q^{*2}(w^* + 1)^3} + \frac{ac\beta(1 - f)(\delta - q^*)p^*}{q^{*2}(w^* + 1)^2(p^* + 1)^2} > 0.
\end{aligned}$$

Then Hurwitz criteria implies that all the roots of (3.19) has the real parts with negative signs if

$$\mathrm{Det}_0 < 0, \tag{3.20}$$

and has the real parts with positive signs if (3.20) is violated.

Then, we have the following conclusion about the stability of equilibria.

Theorem 3.5. *Assume that* $c > 1$. *For the equilibria of model* (2.7), *we have the following results.*

(1) The boundary equilibrium $E^0(w^0, q^0, 0)$ *is locally asymptotically stable provided* $\mathcal{R}_0 < 1$ *and unstable provided* $\mathcal{R}_0 > 1$. *In particular, when* $1 < \delta < \frac{c}{c-1}$, *it is globally asymptotically stable.*

(2) Any positive equilibrium $E^*(w^*, q^*, p^*)$, *if exists, is locally asymptotically stable provided* $\mathrm{Det}_0 < 0$ *and unstable provided* $\mathrm{Det}_0 > 0$.

3.4. Bifurcation analysis

It follows from Theorems 3.3 and 3.5 that when $\mathcal{R}_0 < 1$, model (2.7) may show the coexistence between a boundary equilibrium and two positive equilibria. To identify this dynamic property, we explore possible bifurcations that model (2.7) may undergo. For the convenience, we denote the variables w, q, p in model (2.7) by x_1, x_2, x_3, and $H = (h_1, h_2, h_3)$. The dimensionless precipitation a is taken as the bifurcation parameter.

We first prove the existence of a transcritical bifurcation by using Theorem 4.1 in Castillo-Chavez and Song (2004) (also can refer to Theorem 2.5 in Lan et al. (2021)).

Theorem 3.6. *If* $a = a^* = \frac{cl}{f(\beta\delta(c-1)-\beta c-c)}$, *(i.e.,* $\mathcal{R}_0 = 1$*), then model* (2.7) *undergoes a transcritical bifurcation at* $E^0(w^0, q^0, 0)$, *which is backward provided* $m_1 > 0$ *and forward bifurcation provided* $m_1 < 0$, *where*

$$m_1 = \frac{2(\beta\delta(c-1) - \beta c - c)}{\beta c^2(\delta - 1)} + \frac{2s\beta lf(c-1)(\beta\delta(c-1) - \beta c - c)}{c(f\gamma(\beta\delta(c-1) - \beta c - c) + \beta l(c-1)(f-1))}. \tag{3.21}$$

Proof. It follows from $\mathcal{R}_0 = 1$ that $a = a^*$. From (3.18), it is easy to see that when $a = a^*$, the Jacobi matrix at $(w^0, q^0, 0)$ has a zero simple eigenvalue. For the zero eigenvalue, a right eigenvector is $\mu = (1, \mu_2, \mu_3)^T$ where the superscript T denotes the transpose of a vector and

$$\mu_2 = \frac{(\beta\delta(c-1) - \beta c - c)^2}{\beta c(c-1)^2(\delta - 1)},$$

$$\mu_3 = -\frac{\beta lf(c-1)(\beta\delta(c-1) - \beta c - c)}{c\Big(f\gamma(\beta\delta(c-1) - \beta c - c) + \beta l(c-1)(f-1)\Big)},$$

and a left eigenvector is

$$\nu = (\nu_1, \nu_2, \nu_3) = \Big(0, 0, \frac{1}{\mu_3}\Big).$$

In order to apply Theorem 4.1 in Castillo-Chavez and Song (2004), we need to examine the signs of two quantities m_1, m_2, where

$$m_1 = \sum_{k,i,j=1}^{3} \nu_k \mu_i \mu_j \frac{\partial^2 h_k}{\partial x_i \partial x_j}, \ m_2 = \sum_{k,i=1}^{3} \nu_k \mu_i \frac{\partial^2 h_k}{\partial x_i \partial a}. \tag{3.22}$$

Due to the left eigenvector l, we just need to calculate the second derivatives of h_3. Simple calculations show that

$$\frac{\partial^2 h_3}{\partial x_2 \partial x_3}\Big|_{(w^0,q^0,0)} = \frac{c}{q^2}, \qquad \frac{\partial^2 h_3}{\partial x_3^2}\Big|_{(w^0,q^0,0)} = -2s, \tag{3.23}$$

and the rest of the second derivatives in (3.22) are all zero. Therefore,

$$\begin{aligned} m_1 &= \frac{2(c-1)^2\mu_2}{c} - 2s\mu_3 \\ &= \frac{2(\beta\delta(c-1)-\beta c - c)}{\beta c^2(\delta-1)} + \frac{2s\beta l f(c-1)(\beta\delta(c-1)-\beta c-c)}{c(f\gamma(\beta\delta(c-1)-\beta c-c)+\beta l(c-1)(f-1))}, \\ m_2 &= \frac{\beta f l(c-1)^2(\delta-q)}{(af+l)((\beta+c)af+cl)} > 0. \end{aligned}$$

Based on Theorem 4.1 in Castillo-Chavez and Song (2004), we immediately obtain that the bifurcation at $\mathcal{R}_0 = 1$ $(a = a^*)$ is backward when $m_1 > 0$ and forward when $m_1 < 0$. □

According to (3.19), it is easy to check that Jacobi matrix J at the positive equilibrium $E^*(w^*, q^*, p^*)$ has a simple zero eigenvalue $\lambda = 0$ when $\mathrm{Det}_0 = 0$, i.e., when

$$a = a^{**} := \frac{\gamma(p^*+1)^2}{\beta(1-f)}\Big(\frac{slq^{*2}((\beta+c)w^*+c)(w^*+1)}{c\gamma(\delta-q^*)} + sq^{*2}p^* + \frac{\beta(\delta-q^*)w^*}{w^*+1}\Big). \tag{3.24}$$

The following theorem shows that a saddle-node bifurcation occurs when a crosses the value a^{**}.

Theorem 3.7. *Assume that* $\delta > \frac{c(\beta+1)}{(c-1)\beta}$ *and* $c > 1$, *and* $E^*(w^*, q^*, p^*)$ *is a positive equilibrium of model* (2.7). *If* $a = a^{**}$ *and* $\widetilde{\Theta} \neq 0$, *then model* (2.7) *undergoes a saddle-node bifurcation at* $E^*(w^*, q^*, p^*)$.

Proof. Let U and V be a right and left eigenvector of Jacobi matrix J corresponding to $\lambda = 0$. Direct calculation yields to

$$U = (U_1, U_2, U_3)^T = \Big(\frac{(\beta w^* + c(w^*+1))(w^*+1)}{\beta(\delta-q^*)}, 1, \frac{c}{sq^{*2}}\Big)^T,$$

$$V = (V_1, V_2, V_3)^T = \Big(1, \frac{l(w^*+1)^2 + \gamma(\delta-q^*)p^*}{\beta(\delta-q^*)}, \frac{a^{**}(1-f)}{sp^*(p^*+1)^2} - \frac{\gamma(\delta-q^*)w^*}{sp^*(w^*+1)}\Big)^T.$$

Also, we have

$$H_a(E^*, a^*) = \Big(\frac{p^*+f}{p^*+1}, 0, 0\Big)^T,$$

and then

$$V^T H_a(E^*, a^*) = \frac{p^*+f}{p^*+1} \neq 0. \tag{3.25}$$

We now need to compute $D^2H(E^*, a^*)(U, U)$, which has the form

$$D^2H(E^*, a^*)(U, U) = \Big(\Theta, \frac{-2(\beta+c)^2 w^* + c(\beta+c)}{\beta(\delta - q^*)}, \frac{2c^2(1-s)}{sq^{*4}}\Big)^T,$$

where

$$\begin{aligned}\Theta =& \frac{2\gamma p^*((\beta+c)w^*+c)^2}{\beta^2(\delta-q^*)} + \frac{2\gamma p^*((\beta+c)w^*+c)}{\beta^2(\delta-q^*)(w^*+1)} - \frac{2c\gamma((\beta+c)w^*+c)}{\beta s q^{*2}(w^*+1)}\\ &+ \frac{2c\gamma w^*}{sq^{*2}(w^*+1)} - \frac{2a^{**}c^2(1-f)}{s^2q^{*4}(p^*+1)^3}\end{aligned}$$

It then follows that

$$\begin{aligned}V^TD^2H(E^*, a^*)(U, U) =& \Theta + \frac{(l(w^*+1)^2 + \gamma(\delta-q^*)p^*)(-2(\beta+c)^2w^* + c(\beta+c))}{\beta^2(\delta-q^*)^2}\\ &+ \frac{2c^2(1-s)}{sq^{*4}}\Big(\frac{a^{**}(1-f)}{sp^*(p^*+1)^2} - \frac{\gamma(\delta-q^*)w^*}{sp^*(w^*+1)}\Big) := \widetilde{\Theta}.\end{aligned}$$

It then follows from Sotomayors theorem (Perko, 1996) that system (2.7) undergoes a saddle-node bifurcation at $E^*(w^*, q^*, p^*)$ when a crosses a^{**}. □

4. Numerical simulations

Notice that soil texture is crucial to the availability of soil water for plants. In general, sandy soil has large gaps and permeability, but poor water retention, low nutrient content, and poor fertility. In contrast, clay soil has small gaps, poor permeability, strong water and fertilizer retention, more organic matter. These soil properties will affect the absorption of water by plants and the transmission and consumption of water in plants to a certain extent. In this paper, we focus on these two soil conditions by setting $f = 0.1$ as sandy soils and $f = 0.9$ as clay soils, and study the impact of climatic factors (precipitation, a) and plant traits (water storage capacity, δ) on the growth of plants. For other parameters appearing in model (2.7), we take the following values according to Table 1:

$$l = 0.5, \gamma = 0.00079, \beta = 0.59, c = 2.5, s = 0.075. \tag{4.1}$$

Water storage capacity is the performance of drought resistance of plant species, which represents a certain kind of plants. The impacts of water storage capacity of plants δ on the soil water, the water in plants, and the plant growth are shown in Fig. 1 by bifurcation analysis. If plants are supported by sandy soil ($f = 0.1$, see the upper row in Fig. 1), model (2.7) undergoes a saddle-node bifurcation at $\delta = 5.790977 := \delta_1$ and a backward bifurcation at $\delta = 8.733055 := \delta_2$, respectively. When $\delta < \delta_1$, model (2.7) only has a 'no-vegetation' state E^0, which is globally asymptotically stable. When $\delta_1 < \delta < \delta_2$, model (2.7) has a 'no-vegetation' state E^0 and two vegetated states E_1^* and E_2^* where $p_1^* < p_2^*$. In this situation, model (2.7) shows a bistability (alternative stable states) between a stable 'no-vegetation' equilibrium and a stable positive equilibrium. When $\delta > \delta_2$, the 'no-vegetation' state becomes unstable, and

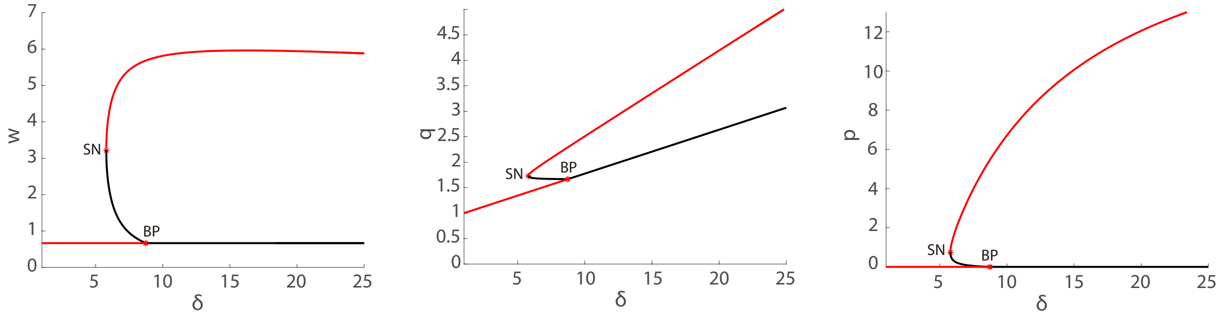

(a) $f = 0.1$

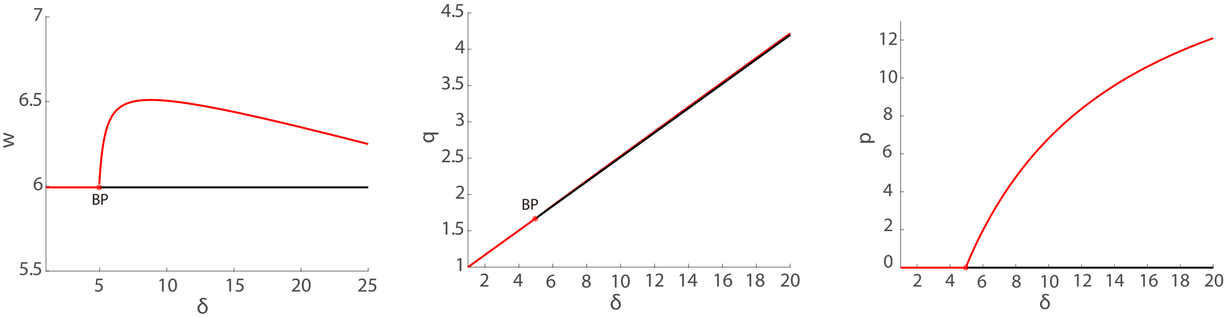

(b) $f = 0.9$

Figure 1: (Color online) Bifurcation diagram of model (2.7) with respect to water storage capacity of plants δ for sandy soil ($f = 0.1$) and clay soil ($f = 0.9$). The other parameters except δ are taken as $a = 3.33$, $l = 0.5$, $\gamma = 0.0079$, $\beta = 0.59$, $c = 2.5$ and $s = 0.075$. The red/black curves denote the stable/unstable equilibria, respectively. The label 'SN' denotes the saddle-node bifurcation and 'BP' the transcritical bifurcation point.

model (2.7) has a unique stable vegetated state. If plants are supported by clay soil ($f = 0.9$, see the lower row in Fig. 1), the dynamics of model (2.7) is quite different from the previous case. Only the forward bifurcation occurs. The bifurcation value of δ is at $\delta = 4.962806 := \delta_3$. When $\delta < \delta_3$, model (2.7) only has a 'no-vegetation' state E^0, which is globally asymptotically stable. When $\delta > \delta_3$, the 'no-vegetation' state becomes unstable, and a positive equilibrium emerges, which is a global attractor.

Fig. 1 is obtained with a precipitation level of $a = 3.33$, which means that the plants are in a relatively dry environment. These results show that the water storage capacity of plants has an important impact on the survival of plants in arid environments, mainly in the following three aspects:

- For plants with weak water storage capacity, due to the relative lack of water resources in arid environments, it is impossible to meet the normal growth needs of plants. Therefore, no matter in sand or clay soil, plants cannot survive, and the plant population will collapse. There is no change in the soil water content in the equilibrium state (the left panel of Fig. 1), because it is assumed that the precipitation is a fixed value, while in the equilibrium state, the plants die, and the soil water will not be consumed.

- There is a critical value of plant water storage capacity in both types of soil, and when the water storage capacity exceeds this critical value, plants begin to have the ability to survive in arid environments. If plants are supported by sandy soil, then in a suitable range of water storage capacity system (2.7) may exhibit a bistable phenomenon. The final plant biomass depends on the initial plant biomass: if the initial vegetation is sparse, then the plants will die out, while if the initial vegetation is luxuriant, then the plants can survive. If plants are supported by clay soil, the bistable behavior does not occur. These indicate that it is very sensitive to different soils for low plant biomass. Due to the low water retention rate of sandy soil, when the biomass is small, plants cannot absorb enough water from the soil to maintain their growth and development, and eventually die. Clay soil, on the other hand, has a high water retention rate, so plants can absorb water from the soil and grow normally.

- For plants with strong water storage capacity, the growth rate of plants in sandy and clay soils will not make much difference due to their strong drought resistance. However, for the water in the soil, the equilibrium density in the sandy soil will not change with the change of water storage capacity, while in the clay, the equilibrium density will decrease with the increase of water storage capacity.

The effect of precipitation on plant growth and development has always been an important topic in plant research. For plants with different water storage capacity, the effect of precipitation may be quite different. Here, we conduct some numerical simulations for the level of water storage capacity of plants $\delta = 6.25$ to explore the influence of precipitation on plants. The corresponding results are shown in Fig. 2. It can be seen that the dynamics of model (2.7) is similar to that in Fig. 1. In extremely dry conditions (i.e., precipitation is very few), plants cannot survive and the plant population collapses. As precipitation gradually increases, the amount of the soil water also increases accordingly. Until the soil moisture reaches a certain amount, plants can survive in arid environments. We mainly consider precipitation as

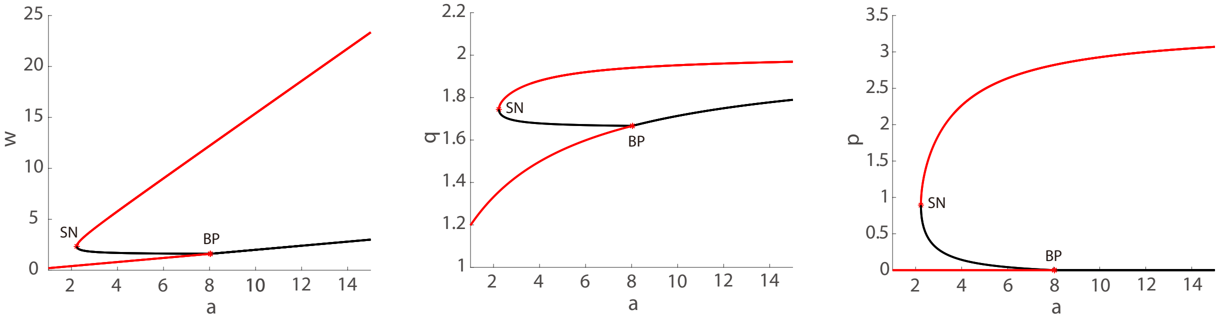

(a) $f = 0.1$

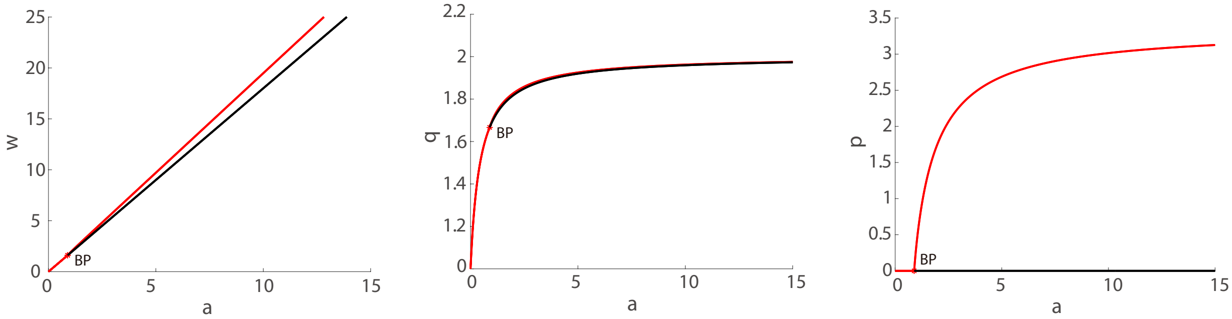

(b) $f = 0.9$

Figure 2: (Color online) Bifurcation diagrams of model (2.7) with respect to the precipitation a for sandy soil ($f = 0.1$) and clay soil ($f = 0.9$). The other parameters except a are taken as $\delta = 6.25$, $l = 0.5$, $\gamma = 0.00079$, $\beta = 0.59$, $c = 2.5$ and $s = 0.075$. The color of the curves and the labels have the same meaning as in Fig. 1.

an indicator to describe the role of precipitation in plant growth. As can be seen from Fig. 2, there is a precipitation threshold, at which model (2.7) has a 'no-vegetation' equilibrium and a positive equilibrium point with multiplicity 2. When precipitation is greater than this threshold, the plants survive, otherwise the plants die. When the climate is relatively humid, the phenomenon of alternative stable states appears. Similar to the impact of water storage capacity, we find that the low plant biomass is very sensitive to the soil types in this humid environment. Compared with sandy soil, clay soil is more favorable for plant colonization with low initial biomass. When the climate is very humid, the plant biomass increases with the increase of precipitation, until the plant biomass reaches a certain amount and no longer increases. At this time, precipitation is no longer a limiting factor for plant growth.

5. Discussion

In order to survive in arid environments, plants have developed some drought resistance strategies, including developed root system and developed water storage tissues, etc. In this paper, we use the method of mathematical modeling to explore the influence of plant water storage capacity on plant growth and development in arid environments. Specifically, we characterize the water storage capacity of plants as the ratio of the maximum and minimum water content in plants. Based on this, a three-variable model describing the dynamics of soil water, water in plants, and plant biomass is proposed. We have investigated the existence and stability of equilibria, and proved that the model may undergo a forward or backward bifurcation and a saddle-node bifurcation.

The bifurcation diagrams illustrate that the soil conditions can significantly affect successful colonization of plants. For plants supported in clay soil, the ecological reproductive index $\mathcal{R}_0$ can be seen as an indicator that the plants can be colonized successfully in the bare areas (see the lower lines in Fig. 1 and Fig. 2). According to the formula $\mathcal{R}_0 = 1$, the critical values of climatic conditions (for example, precipitation) or plant traits (for example, water storage capacity) for plant survival can be determined. In this case, the plant biomass changes slowly with precipitation. For plants supported in sandy soil, it is obvious that $\mathcal{R}_0 = 1$ is not the indicator that the plants can be colonized successfully in the bare areas. The true indicator is dominated by the saddle-node bifurcation point, which is smaller than that determined by $\mathcal{R}_0 = 1$. This critical point is also called tipping point. In addition, it is interesting to note that the plants are resilient to precipitation and water storage capacity for the sandy soil. The result about precipitation is consistent to that in Rietkerk et al. (1997). In appropriate parameter ranges, the phenomenon of alternative stable states may emerge, and the initial plant biomass determines the final plant size. In particular, if the initial biomass of plants is sparse, then they may become extinct. In ecology, this phenomenon is called Allee effect.

In natural ecosystems, especially in arid ecosystems, alternative stable states and tipping points are not uncommon (van Nes et al., 2014, Xu et al., 2020, Hirota et al., 2011, Scheffer et al., 2001). Some studies show that these phenomena are closely related to the degradation and restoration of ecosystems. As the parameter approaches the tipping points, the original stable ecosystem may undergo unpredictable rapid degradation or even collapse in a short time, and the degraded system state also has high stability and is often difficult to recover. On the other hand, these phenomena also can explain some irrational facts in nature, such as the increase of surface runoff in the Sahel region after a long-term severe drought from the 1970s to the mid-1990s (Wendling et al., 2019). In the mechanisms causing these phenomena, drought may be an important factor in arid environments (van Nes et al., 2014, Hirota et al., 2011, Rietkerk et al., 1997). Moreover, Rietkerk et al. (1997) showed that the site-specific properties such as nutrients or soil water availability is very important for the resilience of vegetation change. In this paper, it is interesting to note that plant traits such as water storage capacity also can induce the occurrence of these phenomena. This finding provides us a new way to identify the early warning signals for imminent critical transitions, which plays an important role in maintaining the stability of arid ecosystems.

As noted, the water storage capacity of different types of plants and their seasonal changes are quite different. Since most plants growing in arid regions have the ability to obtain water from deep soil, and their hydraulics are very complex, determining the dynamics of the water storage capacity of plants in arid environments is itself a great challenge. In this paper, we do not directly model the water storage capacity of plants as a state variable, but describe it by the water content in plants. It is shown that the decrease of water storage capacity of plants may have a catastrophic effect on the plant ecosystem, which again proves that the water storage capacity plays a very important role in the drought resistance strategies of plants. Moreover, recent researches have indicated that the response of plants to drought has a lag effect (Rundquist and Harrington, 2000, Wu et al., 2015, Tong et al., 2017, Choubin et al., 2019). When the drought stress is over, although the water and soil conditions have been restored to the conditions suitable for plant growth, the plant functions and various growth indicators cannot be restored immediately, that is, some effects of stress on plants will last for a period of time. Therefore, considering this lag effect in the process of describing the interaction between plants and water will make the model more consistent with the real growth law of plants. We will further consider this in future research.

CRediT authorship contribution statement

Cuihua Wang: Conceptualization, Investigation, Writing - original draft. Hao Wang: Conceptualization, Investigation, Writing - review & editing. Sanling Yuan: Conceptualization, Investigation, Writing - review & editing, Supervision.

Declaration of competing interest

The authors declare that they have no known competing financial interests or personal relationships that could have appeared to influence the work reported in this paper.

Acknowledgments

Sanling Yuan is partially supported by National Natural Science Foundation of China (11671260; 12071293), and Hao Wang is partially supported by Natural Sciences and Engineering Research Council of Canada (Individual Discovery Grant RGPIN-2020-03911 and Discovery Accelerator Supplement Award RGPAS-2020-00090).

Appendix A. Computation of $\mathcal{R}_0$

According to (3.18), we know that the eigenvalues of Jacobi matrix $J(E^0)$ are

$$\lambda_1 = -l < 0, \quad \lambda_2 = -\frac{\beta af}{af + l} - c < 0, \quad \lambda_3 = \frac{\beta caf(\delta - 1)}{\beta\delta af + caf + cl} - 1.$$

It is obvious that the stability of $E^0(w_1, q_1, 0)$ is determined by λ_3. Define

$$\mathcal{R}_0 = \frac{\beta caf(\delta - 1)}{\beta\delta af + caf + cl}.$$

Then $\mathcal{R}_0$ is the ecological reproductive index of plants for model (2.7).

Appendix B. Proof of Lemma 3.4

Proof. The condition $1 < q < \delta$ implies that

$$\frac{\mathrm{d}p}{\mathrm{d}t} = p\Big(c\Big(1 - \frac{1}{q}\Big) - 1 - sp\Big) \le p\Big(c\Big(1 - \frac{1}{\delta}\Big) - 1\Big).$$

It then follows that when $1 < \delta < \frac{c}{c-1}$, we have $\lim_{t\to\infty} p(t) = 0$ for any initial value $p(0) \geq 0$. Accordingly, we have the limiting equation of $w(t)$ in (2.7) as

$$\frac{\mathrm{d}w}{\mathrm{d}\tau} = af - lw,$$

from which we know that for any initial value $w(0) \geq 0$, $\lim_{t\to\infty} w(t) = \frac{af}{l}$. Similarly, we obtain the limiting equation for q as

$$\frac{\mathrm{d}q}{\mathrm{d}\tau} = \frac{\beta af}{af+l}\delta + c - \Big(\frac{\beta af}{af+l} + c\Big)q,$$

from which we immediately have that

$$\lim_{t\to\infty} q(t) = 1 + \frac{\beta af(\delta-1)}{lc + (\beta+c)af} = q^0.$$

The proof is thus completed. $\square$

References

Ahanger, M.A., Morad-Talab, N., Abd-Allah, E.F., Ahmad, P., Hajiboland, R., 2016. Plant growth under drought stress: Significance of mineral nutrients. Water stress and crop plants: a sustainable approach 2, 649–668. doi:`https://doi.org/10.1002/9781119054450.ch37`.

Allen, C.D., Breshears, D.D., McDowell, N.G., 2015. On underestimation of global vulnerability to tree mortality and forest die-off from hotter drought in the anthropocene. Ecosphere 6, 1–55. doi:`https://doi.org/10.1890/ES15-00203.1`.

Allen, C.D., Macalady, A.K., Chenchouni, H., Bachelet, D., McDowell, N., Vennetier, M., Kitzberger, T., Rigling, A., Breshears, D.D., Hogg, E.T., et al., 2010. A global overview of drought and heat-induced tree mortality reveals emerging climate change risks for forests. Forest ecology and management 259, 660–684. doi:`https://doi.org/10.1016/j.foreco.2009.09.001`.

Castillo-Chavez, C., Song, B., 2004. Dynamical models of tuberculosis and their applications. Mathematical Biosciences & Engineering 1, 361. doi:`10.3934/mbe.2004.1.361`.

Čermák, J., Kučera, J., Bauerle, W.L., Phillips, N., Hinckley, T.M., 2007. Tree water storage and its diurnal dynamics related to sap flow and changes in stem volume in old-growth douglas-fir trees. Tree physiology 27, 181–198. doi:`https://doi.org/10.1093/treephys/27.2.181`.

Choubin, B., Soleimani, F., Pirnia, A., Sajedi-Hosseini, F., Alilou, H., Rahmati, O., Melesse, A.M., Singh, V.P., Shahabi, H., 2019. Effects of drought on vegetative cover changes: Investigating spatiotemporal patterns, in: Extreme Hydrology and Climate Variability, pp. 213–222. doi:`https://doi.org/10.1016/B978-0-12-815998-9.00017-8`.

DOdorico, P., Porporato, A., Runyan, C., 2019. Ecohydrology of arid and semiarid ecosystems: an introduction, in: Dryland ecohydrology, pp. 1–27. doi:`https://doi.org/10.1007/978-3-030-23269-6_1`.

Gilad, E., Hardenberg, J.v., Provenzale, A., Shachak, M., Meron, E., 2004. Ecosystem engineers: From pattern formation to habitat creation. Phys. Rev. Lett. 93, 98105.1–98105.4. doi:`https://doi.org/10.1103/PhysRevLett.93.098105`.

Gilad, E., Hardenberg, J.v., Provenzale, A., Shachak, M., Meron, E., 2007. A mathematical model of plants as ecosystem engineers. J. Theoret. Biol. 244, 680–691. doi:`https://doi.org/10.1016/j.jtbi.2006.08.006`.

Gustafson, E.J., Sturtevant, B.R., 2013. Modeling forest mortality caused by drought stress: implications for climate change. Ecosystems 16, 60–74. doi:`https://doi.org/10.1007/s10021-012-9596-1`.

Hartzell, S., Bartlett, M.S., Porporato, A., 2017. The role of plant water storage and hydraulic strategies in relation to soil moisture availability. Plant and Soil 419, 503–521. doi:`https://doi.org/10.1007/s11104-017-3341-7`.

HilleRisLambers, R., Rietkerk, M., van den Bosch, F., Prins, H.H., de Kroon, H., 2001. Vegetation pattern formation in semi-arid grazing systems. Ecology 82, 50–61. doi:`https://doi.org/10.1890/0012-9658(2001)082[0050:VPFISA]2.0.CO;2`.

Hirota, M., Holmgren, M., Van Nes, E.H., Scheffer, M., 2011. Global resilience of tropical forest and savanna to critical transitions. Science 334, 232–235. doi:`10.1126/science.1210657`.

Hu, Y., Schmidhalter, U., 2005. Drought and salinity: a comparison of their effects on mineral nutrition of plants. Journal of Plant Nutrition and Soil Science 168, 541–549. doi:`https://doi.org/10.1002/jpln.200420516`.

Lan, G., Yuan, S., Song, B., 2021. The impact of hospital resources and environmental perturbations to the dynamics of sirs model. Journal of the Franklin Institute 358, 2405–2433. doi:`https://doi.org/10.1016/j.jfranklin.2021.01.015`.

Loladze, I., Kuang, Y., Elser, J.J., 2000. Stoichiometry in producer-grazer systems: linking energy flow with element cycling. Bulletin of mathematical biology 62, 1137–1162. doi:`https://doi.org/10.1006/bulm.2000.0201`.

Manzoni, S., Ahmed, M.H., Porporato, A., 2019. Ecohydrological and stoichiometric controls on soil carbon and nitrogen dynamics in drylands, in: Dryland Ecohydrology, pp. 279–307. doi:`https://doi.org/10.1007/978-3-030-23269-6_11`.

McDowell, N., Pockman, W.T., Allen, C.D., Breshears, D.D., Cobb, N., Kolb, T., Plaut, J., Sperry, J., West, A., Williams, D.G., et al., 2008. Mechanisms of plant survival and mortality during drought: why do some plants survive while others succumb to drought? New phytologist 178, 719–739. doi:`https://doi.org/10.1111/j.1469-8137.2008.02436.x`.

van Nes, E.H., Hirota, M., Holmgren, M., Scheffer, M., 2014. Tipping points in tropical tree cover: linking theory to data. Global change biology 20, 1016–1021. doi:`https://doi.org/10.1111/gcb.12398`.

Perko, L., 1996. Differential Equations and Dynamical Systems. Springer, New York.

Phillips, O.L., Van Der Heijden, G., Lewis, S.L., López-González, G., Aragão, L.E., Lloyd, J., Malhi, Y., Monteagudo, A., Almeida, S., Dávila, E.A., et al., 2010. Drought–mortality relationships for tropical forests. New Phytologist 187, 631–646. doi:`https://doi.org/10.1111/j.1469-8137.2010.03359.x`.

Rietkerk, M., Boerlijst, M.C., van Langevelde, F., HilleRisLambers, R., de Koppel, J.v., Kumar, L., Prins, H.H., de Roos, A.M., 2002. Self-organization of vegetation in arid ecosystems. The American Naturalist 160, 524–530. doi:`https://doi.org/10.1086/342078`.

Rietkerk, M., van den Bosch, F., van de Koppel, J., 1997. Site-specific properties and irreversible vegetation changes in semi-arid grazing systems. Oikos , 241–252.doi:`https://doi.org/10.2307/3546592`.

Rundquist, B.C., Harrington, J.A., 2000. The effects of climatic factors on vegetation dynamics of tallgrass and shortgrass cover. Geocarto Int. 15, 33–38. doi:`https://doi.org/10.1080/10106040008542161`.

Runyan, C.W., DOdorico, P., 2019. Modeling of phosphorus dynamics in dryland ecosystems, in: Dryland Ecohydrology, pp. 309–333. doi:`https://doi.org/10.1007/978-3-030-23269-6\_12`.

Scheffer, M., Carpenter, S., Foley, J.A., Folke, C., Walker, B., 2001. Catastrophic shifts in ecosystems. Nature 413, 591–596. doi:`https://doi.org/10.1038/35098000`.

Singh, D.K., Sale, P.W., 2000. Growth and potential conductivity of white clover roots in dry soil with increasing phosphorus supply and defoliation frequency. Agronomy Journal 92, 868–874. doi:`https://doi.org/10.2134/agronj2000.925868x`.

Snyder, K., Tartowski, S., 2006. Multi-scale temporal variation in water availability: implications for vegetation dynamics in arid and semi-arid ecosystems. Journal of Arid Environments 65, 219–234. doi:`https://doi.org/10.1016/j.jaridenv.2005.06.023`.

Sterner, R.W., Elser, J.J., 2017. Ecological stoichiometry, in: Ecological Stoichiometry. doi:`https://doi.org/10.1515/9781400885695`.

Tong, S., Bao, Y., Te, R., Ma, Q., Ha, S., Lusi, A., 2017. Analysis of drought characteristics in xilingol grassland of northern china based on spei and its impact on vegetation. Mathematical Problems in Engineering 2017. doi:`https://doi.org/10.1155/2017/5209173`.

Wang, H., Garcia, P.V., Ahmed, S., Heggerud, C.M., 2022. Mathematical comparison and empirical review of the monod and droop forms for resource-based population dynamics. Ecological Modelling 466, 109887. doi:`https://doi.org/10.1016/j.ecolmodel.2022.109887`.

Wang, H., Smith, H.L., Kuang, Y., Elser, J.J., 2007. Dynamics of stoichiometric bacteria-algae interactions in the epilimnion. SIAM Journal on Applied Mathematics 68, 503–522. doi:`https://doi.org/10.1137/060665919`.

Waring, R.H., Running, S.W., 1978. Sapwood water storage: its contribution to transpiration and effect upon water conductance through the stems of old-growth douglas-fir. Plant, Cell & Environment 1, 131–140. doi:`https://doi.org/10.1111/j.1365-3040.1978.tb00754.x`.

Wei, Z., Wang, Y., 2015. Responses of plants to drought stress. Science Press, China.

Wendling, V., Peugeot, C., Mayor, A.G., Hiernaux, P., Mougin, E., Grippa, M., Kergoat, L., Walcker, R., Galle, S., Lebel, T., 2019. Drought-induced regime shift and resilience of a sahelian ecohydrosystem. Environmental Research Letters 14, 105005. doi:`https://doi.org/10.1088/1748-9326/ab3dde`.

Wu, D., Zhao, X., Liang, S., Zhou, T., Huang, K., Tang, B., Zhao, W., 2015. Time-lag effects of global vegetation responses to climate change. Global change biology 21, 3520–3531. doi:`https://doi.org/10.1111/gcb.12945`.

Xu, C., Wang, H., Liu, Q., Wang, B., 2020. Alternative stable states and tipping points of ecosystems. Biodiversity Science 28, 1417. doi:`10.17520/biods.2020233`.

Xu, L., Zheng, C., Ma, Y., 2021. Variations in precipitation extremes in the arid and semi-arid regions of china. International Journal of Climatology 41, 1542–1554. doi:`https://doi.org/10.1002/joc.6884`.

Yin, J., DOdorico, P., Porporato, A., 2019. Soil moisture dynamics in water-limited ecosystems, in: Dryland Ecohydrology, pp. 31–48. doi:`https://doi.org/10.1007/978-3-030-23269-6\_2`.